

Momentum Transfer Dependence of the Differential Cross Section for J/ψ Production

E. G O T S M A N¹⁾, E. L E V I N²⁾,
U. M A O R³⁾ and E. N A F T A L I⁴⁾

*School of Physics and Astronomy
Raymond and Beverly Sackler Faculty of Exact Science
Tel Aviv University, Tel Aviv, 69978, ISRAEL*

Abstract: We discuss the $|t|$ dependence of J/ψ production in the region of $0 < |t| \lesssim M_\psi^2$. The forward slope of the elastic differential cross section is calculated assuming a dipole-type dependence for the gluon ladder-proton form factor. The $|t|$ dependence of $d\sigma/dt$ is obtained using DGLAP evolution both for the elastic channel at low $|t|$ and for the inelastic channel at large values of $|t|$, up to $|t| \simeq M_\psi^2$. Results are presented and compared with the relevant experimental data.

¹⁾ Email: gotsman@post.tau.ac.il .
²⁾ Email: leving@post.tau.ac.il .
³⁾ Email: maor@post.tau.ac.il .
⁴⁾ Email: erann@post.tau.ac.il .

1 Introduction

Measurements of high energy exclusive production of J/ψ meson in photon-proton collisions serve as an important testing ground to quantify the “hard” physics of pQCD in the limit of a small scaling variable x . A process is considered to be “hard” if a large momentum scale is involved, so that the leading contribution of the hadronic fluctuation of the photon is a small perturbative $q\bar{q}$ pair. This large momentum scale may be a heavy quark mass, large virtuality of the photon Q^2 or large four momentum transfer squared at the proton vertex ($-t$). For the diffractive photoproduction of J/ψ this hard scale is provided by the charm quark mass. In our recent letter [1] we presented a screened model which yielded impressive agreement with the rich experimental data on high energy J/ψ photoproduction. The model includes contributions of the off diagonal (skewed) gluon distributions [2], as well as the real part of the production amplitude. In addition, we addressed the issue of Fermi motion of the heavy quark within the quarkonium system [3], which provides further suppression of the final cross section. We argued that on one hand this effect is sensitive to the charm quark mass, while on the other hand, in the relevant kinematical region of the experimental data, it has a rather mild energy dependence. An obvious conclusion of the above argument is that with the current theoretical uncertainties regarding the Fermi motion suppression, the benefits resulting from a phenomenological model would be rather small. The correction due to Fermi motion has been estimated as an overall suppression factor of approximately 30%.

In the present work, we present an analysis for the t dependence of the J/ψ differential cross section which is compatible with our recent investigation of the integrated cross section. To compare with the experimental data we need to know B - the J/ψ forward slope of the differential cross section. In [1] we assumed a weak dependence of B on x , which was calculated by averaging the square of the impact parameter b , using our screening correction (SC) formalism [4]. This input assumption is not sufficient for a detailed t dependence study of J/ψ differential cross sections as the presently available preliminary experimental data on B [5] show a steeper energy dependence than our prediction. The goals of the present improved version of our model are, thus, to reproduce the value as well as the energy dependence of B while maintaining the quality of the results achieved in [1].

In our previous study, a b -space Gaussian was assumed for $S(b)$, the gluon ladder-proton non perturbative form factor [1, 4, 6]. After a careful check, it appears that the integrated cross sections [1] and nucleon structure function [6, 7] are not sensitive to the choice of $S(b)$. The impact parameter dependence plays an important role, when calculating screening corrections to heavy nuclei structure functions, where a Wood-Saxon like [8] profile function has been used [9], or for the J/ψ differential photoproduction cross sections [10] which is the main goal of the present study. As we shall demonstrate, the experimental data [5] for the forward differential cross section slope can be well reproduced with the observation that the energy dependence of B is sensitive to the choice of $S(b)$. It appears that the Fourier transform of the dipole

electromagnetic form factor, is the preferred profile for estimating the screening corrections to B .

The momentum transfer t at the proton vertex controls the size of the interacting system, which emits the gluon ladder. The t dependence of hard processes can, thus, be separated into three kinematical zones. The low $|t|$ region, where the transverse size of the interacting system is of the order of $1/Q_0$, where Q_0^2 is the input scale for the DGLAP[11] evolution ($Q_0^2 \sim 1 \text{ GeV}^2$). This region, in which $0 < |t| < Q_0^2$, has been explored experimentally, mainly via elastic processes [12]. The hard scale in this region is determined by the c -quark mass $m_c^2 \approx M_{J/\psi}^2/4$. The second region is the intermediate region $Q_0^2 < |t| < M_\psi^2$. We suggest that the physics of this region is similar to the physics of the small $|t|$ region, *i.e.* the process is still dominated by large logarithms due to momentum integration over loops in the ordered gluon ladder. However, the scale of the initial conditions of the DGLAP evolution is determined by t , as it becomes of comparable size to Q_0^2 . More specifically, the process is dominated by $\log(M_{J/\psi}^2/t)$. In the intermediate region, the vector meson is produced mostly quasi elastically, while the proton dissociates into a diffractive mass. Note that the diffractive t slope is considerably smaller than the elastic one. In the present study we compare our calculations in this region with preliminary experimental data which were read off figures given in Refs. [13, 14]. As $|t|$ increases, the hard process behavior is dominated by the value of $|t|$, the $|t|$ dependence is inverted [15] and the momenta on the gluon ladder are no longer strongly ordered. Consequently, predictions for the cross section cannot be described using conventional DGLAP evolution. This third region of large $|t|$ has not been explored experimentally.

These three regions of $|t|$ were first discussed in [15] by Forshaw and Ryskin and by Bartels, Forshaw, Lotter and Wuesthoff in the framework of the BFKL equation [16], where it was stated that each of the above regions corresponds to different physics. In a later publication [17], a BFKL calculation of vector meson production, and in particular of J/ψ production, was presented and a good description of experimental data was obtained.

In this paper, we suggest a description of the second kinematic region of intermediate $|t|$ ($Q_0^2 < |t| \lesssim M_\psi^2$) using the DGLAP [11] approach, this yields simple and transparent formulae which have explicit matching to the region of small $|t|$.

Our paper is organized as follows: in section 2 we calculate the forward slope for different profiles and compare with the experimental data. In sections 3 and 4 we calculate the differential cross sections for exclusive J/ψ production both in the elastic and the inelastic channels, respectively. Our conclusions are given in section 5.

2 Forward Slope for Differential Cross Section

In this section we calculate the B -slope for J/ψ production, including screening corrections for up to one extra gluon emission. Our formalism for calculating the screening corrections [18]

is based on the iteration of the non-linear evolution equation [19] for the imaginary part of the elastic amplitude for a dipole to scatter off a hadron target, which is valid in the whole kinematic region, including the low x region [20].

The interaction of a dipole with the target is realized through an exchange of gluons. In the target rest frame, one can use Gribov's factorization in the context of a dipole-nucleon interaction: a dipole emits a soft gluon which develops into a ladder by successive emissions of small x gluons. Subsequently, the gluon ladder interacts with the target. At high energies, the transverse size of an interacting dipole does not change during the QCD interaction, and therefore dipoles are good degrees of freedom. In the limit of large number of colors, a leading logarithmic soft gluon wave function is equivalent to a dipole wave function, and thus, the interaction between a dipole and a target can be treated as a process which is subsequent to a transition of a dipole into two dipoles. Consider a decay of a dipole with transverse size r_\perp into two dipoles as shown in Fig. 1. The probability for this decay is given by the square of the wave function of the dipole. At large N_c one can view this decay as an emission of a zero transverse size gluon. In this framework, the cross section for the virtual photon-nucleon interaction is written as

$$\sigma_{tot}(\gamma^*p) = \int d^2r_\perp \int dz \left| \Psi^{\gamma^*}(Q^2; r_\perp, z) \right|^2 \sigma_{dipole}(r_\perp, z) \quad (1)$$

where the wave functions of the virtual photon are well known, in particular the transverse wave function is given by the Bessel function K_1 . In our model, the dipole-nucleon cross section consists of two contributions:

1. The first, denoted $\hat{\sigma}^q(r_\perp)$, is the percolation of a $q\bar{q}$ pair through the target, without taking into account the extra gluon, and it is calculated using a multi gluon ladder exchange. This contribution can be expressed as a product of the dipole wave function and the cross section for the dipole to scatter off the nucleon. In impact parameter space, $\hat{\sigma}^q$ can be written in the form [18, 21]

$$\hat{\sigma}^q(r_\perp) \propto \int d^2b_\perp d^2r_\perp K_1(\bar{Q}r_\perp) \left(1 - e^{-\frac{1}{2}\Omega_q}\right), \quad (2)$$

where $\bar{Q} = (Q^2 + M_\psi^2)/4$, $x = (Q^2 + M_\psi^2)/W^2$ and the opacity $\Omega_q = \Omega_q(b, r_\perp, x)$ is defined as

$$\Omega_q = \Omega_q(b, r_\perp, x) = \frac{\pi^2}{3} r_\perp^2 \alpha_s \left(\frac{4}{r_\perp^2} \right) xG \left(x, \frac{4}{r_\perp^2} \right) S(b_\perp). \quad (3)$$

The b_\perp dependence of Ω_q is expressed through the profile function $S(b_\perp)$, which we shall discuss later. Note that the argument of the Bessel function should be ar_\perp , where $a^2 = z(1-z)Q^2 + M_\psi^2/4$, however, for heavy quarks, we use the approximation $z = \frac{1}{2}$.

2. For the second contribution, denoted $\hat{\sigma}^g(r_\perp)$ below, we consider an additional gluon in the hadronic state which percolates through the target. We assume that the parent dipole

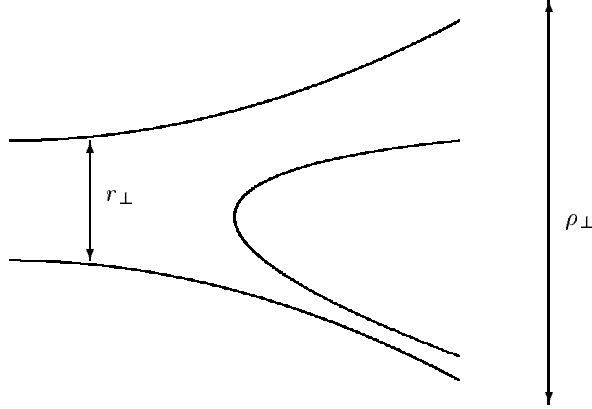


Figure 1: A decay of one dipole with transverse size r_\perp into two dipoles. In the case where two of the produced quarks are with small transverse separation, they can be view as a zero transverse size gluon, hence the final state is a $q\bar{q}g$ state.

whose transverse size is r_\perp , is larger than the produced dipole whose transverse size is ρ_\perp (see Fig. 1). The second contribution can be written in the form [18, 21]:

$$\hat{\sigma}^g(r_\perp) \propto \int d^2b_\perp d^2r_\perp K_1(\bar{Q}r_\perp) \frac{C_F}{\pi^2} \alpha_s r_\perp^2 \int \frac{dx}{x} \int_{\rho_\perp > r_\perp} \frac{d^2\rho_\perp}{\rho_\perp^4} (1 - e^{-\frac{1}{2}\Omega_g}), \quad (4)$$

with $\Omega_g(b, r_\perp, x) = \frac{9}{4}\Omega_q(b, r_\perp, x)$.

The forward slope B is given by [22]:

$$B = \frac{1}{2} \langle b_\perp^2 \rangle = \frac{\int b_\perp^2 db_\perp^2 S(b_\perp)}{2 \int db_\perp^2 S(b_\perp)}, \quad (5)$$

where the factor of one half is introduced since B is measured for cross sections rather than amplitudes. To calculate the forward slope B , we need to average over the impact parent b_\perp , using the sum of (2) and (4) as weights,

$$B = \frac{\int d^2b_\perp d^2r_\perp b_\perp^2 K_1(\bar{Q}r_\perp) \left[(1 - e^{-\frac{1}{2}\Omega_q}) + \frac{C_F}{\pi^2} \alpha_s r_\perp^2 \int \frac{dx}{x} \int_{\rho_\perp > r_\perp} \frac{d^2\rho_\perp}{\rho_\perp^4} (1 - e^{-\frac{1}{2}\Omega_g}) \right]}{2 \int d^2b_\perp d^2r_\perp K_1(\bar{Q}r_\perp) \left[(1 - e^{-\frac{1}{2}\Omega_q}) + \frac{C_F}{\pi^2} \alpha_s r_\perp^2 \int \frac{dx}{x} \int_{\rho_\perp > r_\perp} \frac{d^2\rho_\perp}{\rho_\perp^4} (1 - e^{-\frac{1}{2}\Omega_g}) \right]}. \quad (6)$$

Being the root mean square average in b_\perp space, B is sensitive to the b_\perp dependence of the opacities Ω_q and Ω_g , which depend on $S(b_\perp)$.

The profile functions $S(b_\perp)$ are connected to the form factors via Fourier transforms. We have investigated three different form factors listed below, and compared the results with the relevant experimental data on the J/ψ forward slope [5].

1. An exponential form factor,

$$F_{exp}(t) = e^{\frac{1}{4}R^2t}, \quad (7)$$

which transforms into a Gaussian in impact parameter space.

2. An electromagnetic form factor

$$F_{dipole}(t) = \frac{1}{(1 - \frac{1}{8}R^2t)^2}, \quad (8)$$

its Fourier transform in b_\perp space is

$$S(b_\perp) = \frac{1}{\pi R^2} \frac{\sqrt{8}b_\perp}{R} K_1\left(\frac{\sqrt{8}b_\perp}{R}\right). \quad (9)$$

3. For completeness, we have also investigated the form factor, suggested in [23],

$$F_{DL}(t) = \frac{4m_p^2 - 2.79t}{4m_p^2 - t} \frac{1}{(1 - t/0.71)^2}, \quad (10)$$

where m_p is the proton's mass. The Fourier transforms of F_{DL} is given by,

$$S(b_\perp) = \frac{1}{4\pi} \left[a_1 \left(K_0(\sqrt{0.71}b_\perp) - K_0(2m_p b_\perp) \right) + a_2 b K_1(\sqrt{0.71}b_\perp) \right], \quad (11)$$

where the values of $a_1 \approx 0.8$ and $a_2 \approx 0.33$ were calculated from the numerical coefficients in (10).

The various coefficients are determined from the normalization condition $\int d^2b_\perp S(b_\perp) = 1$.

In our calculations we have substituted each of the above mentioned profiles in (6), and calculated B for the three different PDF parameterizations [24, 25, 26] for the gluon distribution which appears in (3). Our results are shown in Fig. 2. While the energy dependence obtained using F_{dipole} and F_{DL} is in agreement with the ZEUS data, the Gaussian distribution predicts an increase with energy which is too mild to reproduce the measured slope. Regarding normalization, the data is well reproduced by (9) with the choice $R^2 = 10 \text{ GeV}^{-2}$. However, some adjustments are needed regarding the numerical parameters of (11). The choice of our single parameter, is comparable with our earlier estimations ($R^2 = 8.5 \text{ GeV}^{-2}$), where we used a Gaussian distribution for $S(b_\perp)$, and we maintain the quality of our results presented in Ref. [1].

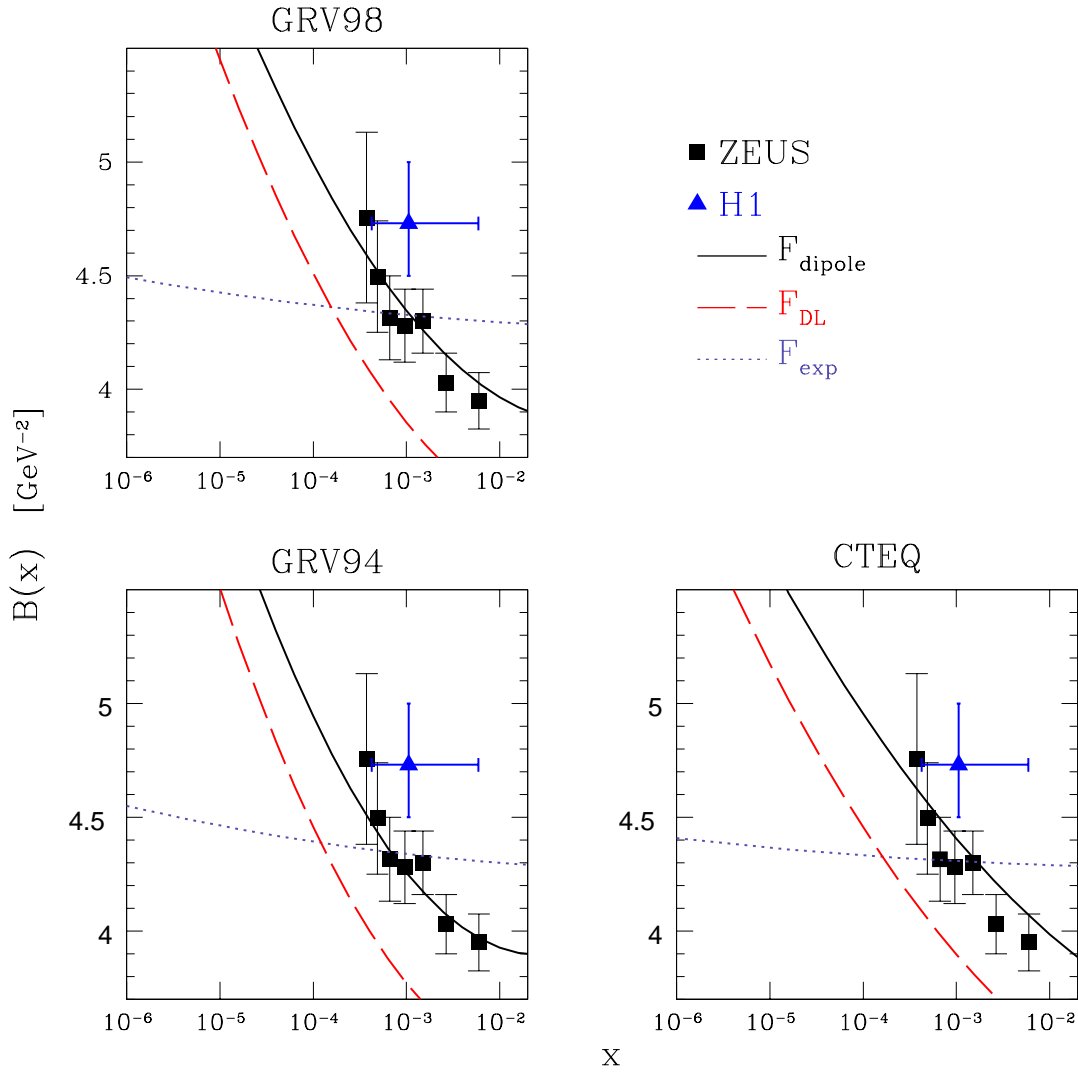


Figure 2: The forward slope for differential cross section of J/ψ production, data and predictions, corresponding to different profile functions $S(b_{\perp})$. Predictions have been calculated for three different PDFs.

3 Differential Cross Section at Low $|t|$

In this section we calculate $d\sigma/dt$ as a function of t for the region of $|t| < Q_0^2$, where Q_0^2 is the scale at which the input for the evolution is computed. Our expressions are based on a simplified model of two Pomeron exchange, which we find to be satisfactory, given the sizeable experimental errors, although our screening correction formalism is capable of deriving a full series calculation. It should be appreciated that what follows in this section is a very simplified picture of screening corrections to the lowest order and it should not be used for calculating other physical quantities, *e.g.* integrated cross sections, on which more accurate data exist.

The procedure for calculating the forward differential cross section for photo production of a heavy vector meson in the color dipole approximation is straightforward [27]. We follow [1] and write the differential cross section at $t = 0$, in the leading logarithmic approximation of pQCD, including a contribution from the real part of the production amplitude [28] and the skewed (off diagonal) gluon distribution,

$$\frac{d\sigma(\gamma p \rightarrow Vp)}{dt} = \frac{16\pi^3 \Gamma_{ee}}{3\alpha_{em} M_V^2} \left(\frac{2^{2\lambda+3} \Gamma(\lambda + \frac{5}{2})}{\sqrt{\pi} \Gamma(\lambda + 4)} \right)^2 \left\{ 1 + \tan^2\left(\frac{\pi\lambda}{2}\right) \right\} \alpha_s^2(\bar{Q}) x G^2(x, \bar{Q}^2), \quad (12)$$

where $\lambda = \partial \log xG / \partial \log(1/x)$. In the derivation of (12), a simple static non relativistic estimate of the vector meson wave function was used. As stated [1], we consider the correction due to Fermi motion, which changes the numerical value obtained from the above equation, by an overall (constant) suppression factor.

In [1] we took into account further suppression of (12) due to screening. These are facilitated by damping factors [6, 29] which are the ratios of the screened to non screened observables. Specifically, the DLLA contributions to the damping factors, are due to screening in the quark sector (denoted D_q) and in the gluon sector (denoted D_g). The DLLA screening correction calculation, was derived in [29] using a Gaussian distribution for the profile $S(b_\perp)$ [see Eq. (7)]. For completeness, we briefly described the basic formulae.

The damping factor due to the screening in the quark sector *i.e.* the percolation of the $c\bar{c}$ through the target, is:

$$D_q^2 = \left(\frac{1}{\kappa_q} E_1\left(\frac{1}{\kappa_q}\right) e^{\frac{1}{\kappa_q}} \right)^2, \quad (13)$$

where κ_q is given by

$$\kappa_q = \frac{2\pi\alpha_S}{3R^2\bar{Q}^2} x G^{DGLAP}(x, \bar{Q}^2). \quad (14)$$

Our expression for the damping in the gluon sector, is the square of the gluon damping defined in [6, 7],

$$xG^{SC}(x, Q^2) = D_g(x, Q^2) xG^{DGLAP}(x, Q^2), \quad (15)$$

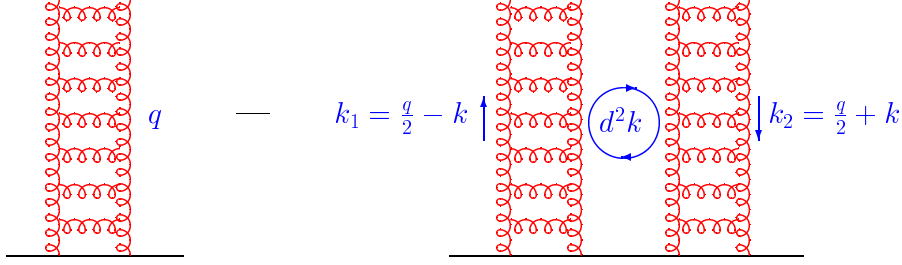


Figure 3: The first two contributions to the amplitude.

where

$$xG^{SC}(x, Q^2) = \frac{2}{\pi^2} \int_x^1 \frac{dx'}{x'} \int_0^{Q^2} dQ'^2 \int db^2 \left(1 - e^{-\kappa_g(x', Q'^2; b^2)}\right), \quad (16)$$

and $\kappa_g = \frac{9}{4}\kappa_q$. The overall damping factor for (12) is $D^2(x, Q^2) = D_q^2(x, Q^2)D_g^2(x, Q^2)$.

Since the opacities used in (13)-(16) for calculating $D^2(x, Q^2)$ were calculated using a Gaussian profile, we examined the sensitivity of $D^2(x, Q^2)$ to the choice of $S(b_\perp)$, so as to validate our normalization for the $t = 0$ differential cross section which had been used for calculating the integrated cross section. The result of our calculations show that replacing a Gaussian profile with (9) leads to a change of D^2 which is less than 4%. We thus conclude that as far as screening corrections are concerned, we can safely rely on our previous estimations at $t = 0$.

Eq. (2) and Eq. (4) can be viewed as the exchange of many “hard” Pomerons (gluon ladders). In the region of small $|t|$ we approximate this process by the exchange of one and two “hard” Pomerons (see Fig. 3). The t -dependence of a single Pomeron exchange amplitude is proportional to $e^{\frac{1}{2}B(W)t}$. The exchange of two “hard” Pomerons leads to an integration over d^2k :

$$\int d^2k e^{\frac{1}{2}B(W)((\frac{\bar{q}}{2} - \vec{k})^2 + (\frac{\bar{q}}{2} + \vec{k})^2)} \rightarrow e^{\frac{1}{4}B(W)t}$$

where $t = -q^2$. Hence, in Fig. 3 the first diagram is proportional to $e^{\frac{1}{2}B(W)t}$ and the second diagram is proportional to $e^{\frac{1}{4}B(W)t}$.

We therefore approximate the differential cross section as the sum of these two exchanges *i.e.*,

$$\frac{d\sigma(W, t)}{dt} = A_{el}^2 \left(e^{\frac{1}{2}B(W)t} - \eta e^{\frac{1}{4}B(W)t} \right)^2. \quad (17)$$

We fix our normalization factors A_{el}^2 and η by the requirement that at $t = 0$, Eq. (12) and Eq. (17), once screening corrections as well as Fermi suppression are taken into account, match.

Comparing (12) and (17) including these corrections we find:

$$\begin{aligned}
A_{el}^2(x, \overline{Q}^2) &= K_f \frac{16\pi^3 \Gamma_{ee}}{3\alpha_{em} M_V^2} \left(\frac{2^{2\lambda+3} \Gamma(\lambda + \frac{5}{2})}{\sqrt{\pi} \Gamma(\lambda + 4)} \right)^2 \left\{ 1 + \tan^2\left(\frac{\pi\lambda}{2}\right) \right\} \alpha_s^2(\overline{Q}^2) x G^2(x, \overline{Q}^2), \\
\eta(x, \overline{Q}^2) &= 1 - D(x, \overline{Q}^2),
\end{aligned}
\tag{18}$$

where K_f is the Fermi motion normalization factor.

We calculate $d\sigma/dt$ using (17) and (18) for low values of t , and compare the numerical calculations with the experimental data for elastic exclusive J/ψ production [12]. Note that our model, as presented in (17)-(18), contains no additional parameters. Specifically, the normalization at $t = 0$ is taken from the integrated cross section data [1], and B is taken from section 2. Our results are shown in Fig. 4. The shaded areas in Fig. 4 correspond to the numerical calculations of (17) at each energy range given by Ref. [12], and the dashed lines were calculated by putting $\eta = 0$ in (17). It can be seen that a single-term exponential expression cannot describe the experimental data without modification to the overall normalization, which, as stated, is taken from rich data of integrated cross section. On the other hand, the reproduction of the data is reasonably good, when considering both terms of Eq. (17).

It is interesting to examine numerically the relative role of the first and second contributions of (17). Squaring the ratio between the second term and the first term we have $\eta^2 e^{\frac{1}{2}B(W)|t|}$, which is not only an increasing function of $|t|$ but also an increasing function of W , since both B and η increase with the energy. Hence, the second term becomes more and more important as $|t|$ and/or W increase. According to our calculations, at $t = 0$ the contribution of the second term to the differential cross section varies from 4% at $W = 50 \text{ GeV}^2$ to 10% at $W = 150 \text{ GeV}^2$. At $|t| \approx Q_0^2$ both the first and the second terms of (17) are numerically larger than the value of $d\sigma/dt$, where the second term is 20(60)% from the first term at low (high) center of mass energy.

As the theoretical uncertainties are difficult to estimate, we used the experimental errors to calculate the deviation of our simplified model from the data. The corresponding $\chi^2/\text{n.d.f}$ for the entire measured energy range is 0.7. As in [1], our parameters are strongly constrained by the experimental data.

4 Differential Cross Section at Intermediate $|t|$

The inelastic contribution to the cross section becomes more and more important as the momentum transfer increases. The exponential t dependence (17) was written using the elastic forward slope derived in section 2, which is compatible with the experimental data. In this section we would like to suggest a simple expression for the inelastic differential cross section.

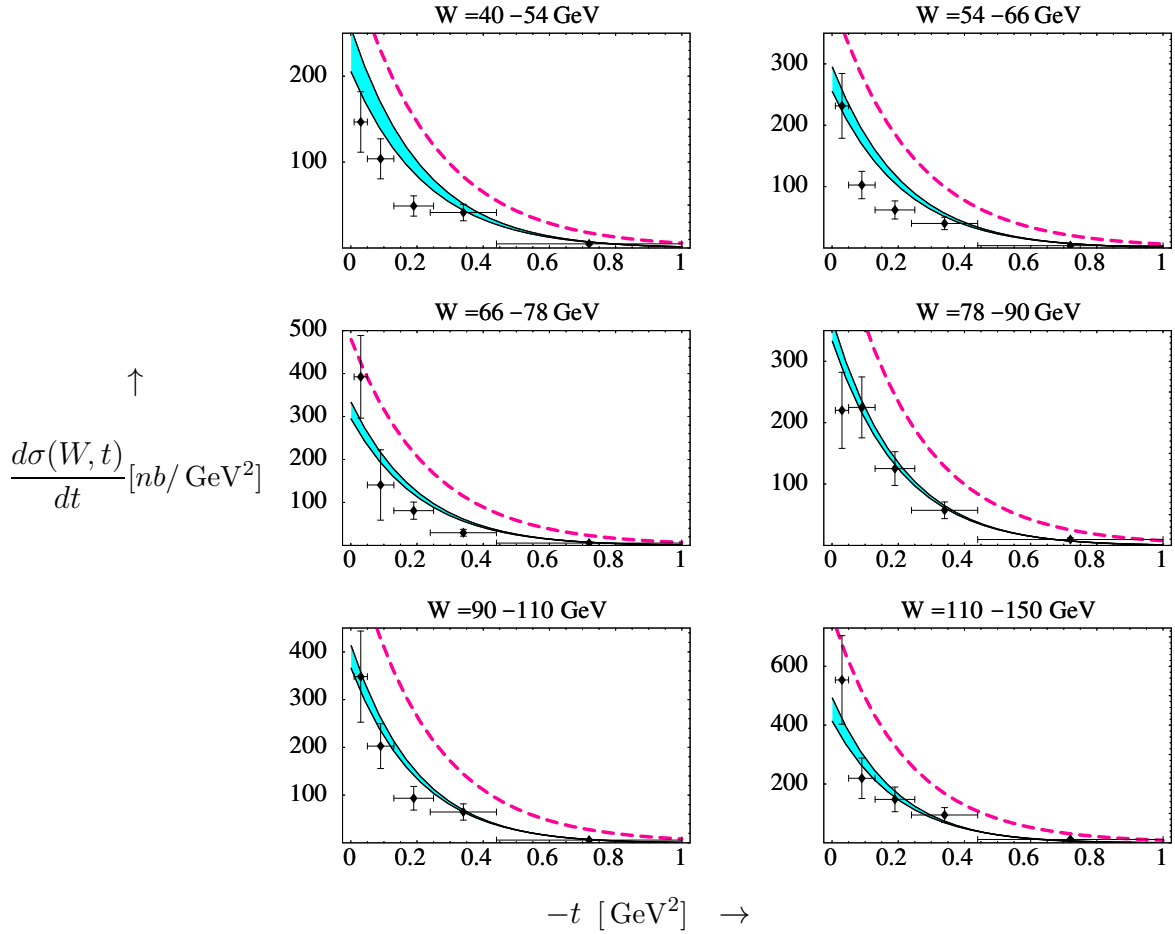


Figure 4: Elastic differential cross section at small t for different energy ranges. The shaded areas correspond to each energy range, as given by Ref. [12], the dashed lines correspond to a single-term exponential form, as further detailed in the text.

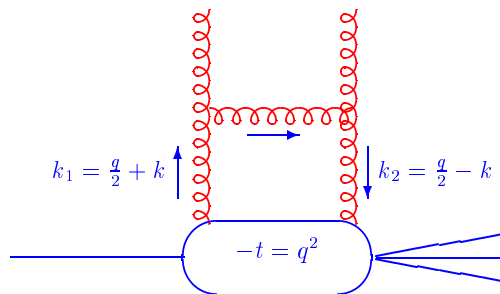


Figure 5: The proton vertex at $-t > Q_0^2$.

As stated in the introduction, hard processes can be calculated using the DGLAP equation, provided the scales of the interaction are such that the momenta on the gluon ladder are ordered. The production of a heavy vector meson can be viewed as the exchange of a gluon ladder between a nucleonic target and vector meson, which is a $q\bar{q}$ system of small transverse size ($\sim 1/M_V^2$). For intermediate values of $|t|$, the momenta are still ordered on the ladder, hence we argue that the DGLAP evolution continues to play a role up to $|t|$ of the order of M_V^2 . Specifically, we can write the amplitude of the lowest rung of the ladder at the proton vertex (see Fig. 5) using the two gluons propagators k_1^{-2} and k_2^{-2} . The corresponding amplitude is proportional to:

$$\frac{(k_1) \cdot (k_2)}{(k_1)^2(k_2)^2}, \quad (19)$$

where $k_1 = (q/2 + k)$, $k_2 = (q/2 - k)$ and the factor $k_1 \cdot k_2$ is implied by gauge invariance. From (19) one can see that the dominant contribution to the evolution equation comes from large logarithms which appear when $k^2 > q^2/4 = -t/4$. For $|t|$ which is not too large, *i.e.* in the intermediate region, the DGLAP equation is still valid for calculating the production amplitude utilizing a gluon distribution function which evolves from $-t/4$ rather than from Q_0^2 .

The physical interpretation of the above discussion is simple. At small $|t|$ ($< 1/m_p^2$) the size of the target is roughly the proton size, the “evolution range” is large and the evolved gluon distribution consists of a large number of gluons. At higher values of momentum transfer the effective size of the target is of the order of $1/|t|$. This leads to a smaller number of emitted gluons, or in other words to a smaller numerical value of xG .

From Eq. (12) we note that the differential cross section is determined by xG . The gluon distribution is related to the numerical value of the opacities, thereby to the screening corrections to the process. Thus, the main t dependence of the process comes from the scale from which the gluon distribution evolves.

Based on the above discussion, we propose the following expression for the differential cross

$W \approx 100 \text{ GeV}$

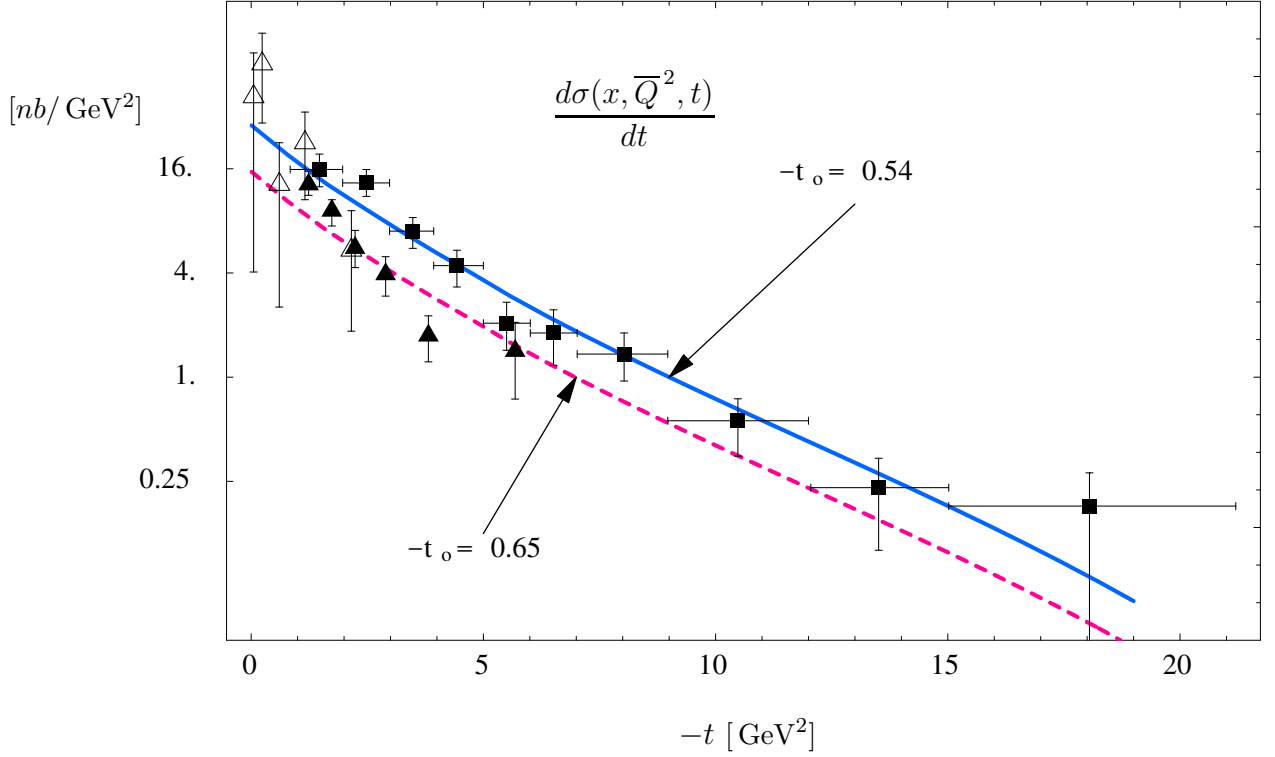


Figure 6: Inelastic differential cross section in the intermediate region of $|t|$. Our calculations are presented, for two different values of the free parameter t_0 , together with the experimental data of H1 preliminary (squares), ZEUS 1995 (open triangles) and ZEUS preliminary (solid triangles)

section:

$$\frac{d\sigma(x, \bar{Q}^2, t)}{dt} = A_{in}^2 D^2(x, \bar{Q}^2, t) x G^2(x, \bar{Q}^2, t) \quad (20)$$

where,

$$xG(x, \bar{Q}^2, t) = xG\left(x, \frac{\bar{Q}^2}{1 + \frac{t}{4\bar{Q}_0^2}}\right), \quad (21)$$

$$x = \frac{Q^2 + M_\psi^2 - t}{W^2} \quad (22)$$

and $D(x, \bar{Q}^2, t)$ is calculated by substituting (21) in (3) and carrying out the screening corrections procedure [1] in both sectors.

The justification for choosing the particular dependence of variables that the gluon distribution depends on is to incorporate its dependence on t . Eq. (21) is written in a typical dimensional

form, *i.e.* the second argument of the gluon distribution has dimensions of GeV^2 . This form is useful for most of the available parameterizations [24, 25, 26], where each parameterization evolves from a slightly different scale Q_0^2 . Since the DGLAP evolution is manifested by logarithms of Q^2/Q_0^2 , the gluon distribution function has a dimensionless form. Our ansatz may be better understood by considering a non-dimensional form of (21), namely $xG(x, \overline{Q}^2/(Q_0^2+|t|/4))$ were it can be seen that as $|t|$ increases, it dominates the scale of evolution whereas at small $|t|$ the gluon distribution function coincide with $xG(x, \overline{Q}/Q_0^2)$.

In (20), the coefficient A_{in}^2 is determined by a continuity requirement, that (17) and (20) match at $t = t_0$, where t_0 is our separation parameter. The results of the numerical calculations, for two different values of t_0 , are shown in Fig. 6, together with the H1 and ZEUS data which have been read off the plot in [13] and [14], respectively. As can be seen from Fig. 6 the large $|t|$ preliminary data set of ZEUS [14] is below the H1 preliminary data [13].

Our calculations of Eq. (20) depends on the fitted value of our free separation parameter t_0 . The upper curve shown in Fig. 6 corresponds to $|t_0| = 0.54 \text{ GeV}^2$, at which A_{in}^2 has been determined to reproduce the H1 data with $\chi^2/\text{n.d.f} = 0.65$. However, as the preliminary sets of H1 and ZEUS data are consistently different, the task of finding a satisfactory description of both sets using the same parameters is not trivial. The best χ^2 for the ZEUS data is obtained with $|t_0| = 0.65 \text{ GeV}^2$ (the lower curve of Fig. 6) where we calculated $\chi^2/\text{n.d.f} = 1.53$. Note that the difference between the two fitted values of t_0 reflects the presumed difference between the H1 and ZEUS sets. This is not necessarily a genuine difference and may just be a consequence of different cuts applied at the diffractive proton vertex, by the two collaborations.

At first sight, it looks as if (20) may affect the results of our previous publication[1], *inter alia* on account of the t -dependence of screening corrections at high $|t|$. However, this effect is compensated by the value of the forward slope, which we calculate using the dipole electromagnetic form factor, as opposed to an exponential form factor used in [1]. Indeed, we found that we still reproduce all the available experimental data. The compensation is so accurate, that the two curves practically overlap, and we have the same χ^2 values as given in [1].

5 Summary and Conclusions

In this paper we have explored the momentum transfer dependence of exclusive production of J/ψ vector mesons. By using a Fourier transform of an electromagnetic form factor as the profile function in the impact parameter space, we calculated the forward differential cross section slope.

We used the expression derived for the slope and calculated the differential cross section for the elastic production of J/ψ by using a simple exponential expression approximating one and two Pomeron exchange.

For the inelastic process, we calculated the differential cross section as a function of t , based on a somewhat naive picture of the interaction. In which we suggested replacing the argument of the gluon distribution so as to obtain a decreasing function of $|t|$, which coincides with pQCD calculations at small $|t|$.

Our conclusions are:

1. The value of the B slope is sensitive to the choice of the profile function $S(b_{\perp})$. Our calculations of B reproduce the experimental data and are not sensitive to the choice of the PDF.
2. The fact that the screening correction formalism with a dipole-type b_{\perp} dependence (F_{dipole}) reproduces both the value and the energy dependence of the t -slope, is important for the understanding of the energy dependence of the “hard” Pomeron trajectory. The contributions of the screening corrections increase with energy and therefore α'_{eff} , the effective slope of the “hard” Pomeron trajectory, should also increase with energy. This result is particular to a screening corrections approach and is not obtained in non-screened pQCD calculations.
3. The screening corrections, which we express through the damping factor D are not effected by a change in the b dependence of the opacities.
4. An exponential form of the differential cross section, which is in agreement with the experimental fits to the forward slope, is suitable for reasonable description of the elastic, low $|t|$, experimental data. This form consists of the first two terms of a multi Pomeron exchange, which are supplemented by screening corrections, as well as corrections due to Fermi motion of the quarks within the charmonium system. This approximation is also valid for describing the integrated cross section.
5. At intermediate values of $|t|$, inelastic data are well reproduced by pQCD which is based on DGLAP evolution. The value of $|t|$ at which the inelastic processes are comparable with elastic processes is $-t_0 \approx 0.5 \text{ GeV}^2$.
6. At intermediate values of $|t|$ the screening corrections dependence on t reflects the decrease of the gluon distribution function.

Acknowledgments

We wish to thank E. Ferreira, who participated in the preliminary stages of this investigation, for his contribution and comments. E.G. wishes to acknowledge the hospitality of the Theoretical Nuclear Physics Group at BNL, where part of this work was done. E.L. thanks the Theory

Group at DESY for the stimulating environment provided while U.M. is indebted to LAFEX at CBPF (Rio de Janeiro) for their support. This research was supported by the BSF grant # 9800276, by the GIF grant # I-620-22.14/1999 and by the Israel Science Foundation, founded by the Israel Academy of Science and Humanities.

References

- [1] E Gotsman, E.M Levin, U. Maor, E Ferreira and E Naftali, *Phys. Lett.* **B503** (2001) 277.
- [2] A.G Shuvaev, K.J Golec-Biernat, A.D Martin and M.G Ryskin, *Phys. Rev.* **D60** (1999) 014015;
A Freund and V Guzey: *Phys. Lett.* **B462** (1999) 178.
- [3] L Frankfurt, W Koepf and M Strikman, *Phys. Rev.* **D54** (1996) 3194.
- [4] E. Gotsman, E.M. Levin and U. Maor: *Phys. Lett.* **B403** (97) 120.
- [5] A. Bruni, talk given at the 8th International Workshop on Deep Inelastic Scattering and QCD, Liverpool, England 2000.
- [6] E Gotsman, E.M Levin, U. Maor and E Naftali, *Nucl. Phys.* **B539** (1999) 535.
- [7] E Gotsman, E.M Levin, U. Maor, E Ferreira and E Naftali, *Phys. Lett.* **B500** (2001) 87.
- [8] H.A. Enge: “*Intr. to Nuclear Physics*”, Addison-Wesley Pub., Mass.,1971.
- [9] E. Gotsman, E. Levin, M. Lublinsky, U. Maor, E. Naftali and K. Tuchin, To appear in ‘The THERA Book’, hep-ph/0101344.
- [10] S. Munier, A. M. Stasto and A. H. Mueller, *Nucl. Phys.* **B603** (2001) 427.
- [11] V.N. Gribov and L.N. Lipatov, *Sov. J. Nucl. Phys.* **15** (1972) 438;
L.N. Lipatov, *Yad. Fiz.* **20** (1974) 181;
G. Altarelli and G. Parisi, *Nucl. Phys.* **B126** (1977) 298;
Yu.L. Dokshitser, *Sov. Phys. JETP* **46** (1977) 641.
- [12] H1 Collaboration, *Phys. Lett.* **B483** (2000) 23.
- [13] D. Brown (H1 collaboration), talk given at the 9th International Workshop on Deep Inelastic Scattering, Italy 2001;
A. Meyer (H1 collaboration), talk on behalf of H1 and ZEUS, given at International Eu-rophysics Conference on High Energy Physics, Budapest 2001;

- H1 collaboration, contributed paper 806, International Europhysics Conference on High Energy Physics, Budapest 2001;
P. J. Bussey, DESY-01-197, hep-ph/0109254, accepted for publication in *Int. J. Mod. Phys. A*.
- [14] ZEUS collaboration, contributed paper 556, International Europhysics Conference on High Energy Physics, Budapest 2001.
- [15] J. R. Forshaw and M. G. Ryskin, *Z. Phys.* **C68** (1995) 137;
J. Bartels, J. R. Forshaw, H. Lotter and M. Wuesthoff, *Phys. Lett.* **B375** (1996) 301.
- [16] E.A. Kuraev, L.N. Lipatov and V.S. Fadin, *Sov. Phys. JETP* **45** (1977) 199;
Ia.Ia. Balitsky and L.N. Lipatov, *Sov. J. Nucl. Phys.* **28** (1978) 822;
L.N. Lipatov, *Sov. Phys. JETP* **63** (1986) 904.
- [17] J.R. Forshaw and G. Poludniowski hep-ph/0107068
- [18] E. Gotsman, E.M. Levin and U. Maor, *Nucl. Phys.* **B493** (1997) 354 and references therein;
E. Gotsman, E. Levin, M. Lublinsky, U. Maor, E. Naftali, K. Tuchin, DESY-00-149, hep-ph/0010198.
- [19] L.V. Gribov, E.M. Levin and M.G. Ryskin, *Phys. Rep.* **100** (1983) 1;
A. H. Mueller and J. Qiu, *Nucl. Phys.* **B 286** (1986) 427;
L. McLerran and R. Venugopalan, *Phys. Rev.* **D 49** (1994) 2233, 3352; **D 50** (1994) 2225, **D 53** (1996) 458, **D 59** (1999) 094002.
- [20] Ia. Balitsky, *Nucl.Phys.* **B 463** (1996) 99;
Yu. Kovchegov, *Phys. Rev.* **D 60** (2000) 034008;
E. Iancu, A. Leonidov and L. McLerran, *Phys.Lett.* **B510** (2001) 133; E. Iancu and L. McLerran, *Phys.Lett.* **B510** (2001) 145.
M. Braun, *Eur. Phys. J.* **C 16** (2000) 337.
- [21] A. H. Mueller, *Nucl. Phys.* **B 335** (1990) 115.
- [22] M. M. Block and R. N. Cahn, *Rev. Mod. Phys.* **57** (1985) 563.
- [23] A. Donnachie and P. V. Landshoff, *Phys. Lett.* **B470** (1999) 243.
- [24] M. Gluck, E. Reya and A. Vogt, *Z. Phys.* **C67** (1995) 433.
- [25] M. Gluck, E. Reya and A. Vogt, *Eur. Phys. J.* **C5** (1998) 461.
- [26] CTEQ Collaboration, H.L. Lai *et al.*, hep-ph/9903282.

- [27] M.G. Ryskin, *Z. Phys.* **C57** (1993) 89;
S.J. Brodsky *et al.*, *Phys. Rev.* **D50** (1994) 3134;
M.G. Ryskin, R.G. Roberts, A.D. Martin and E.M. Levin, *Z. Phys.* **C76** (1997) 231;
L. Frankfurt, M. McDermott and M. Strikman, [hep-ph/9812316](#);
A.D. Martin, M.G. Ryskin and T. Tuebner: *Phys. Lett.* **B454** (1999) 339.
- [28] R.J. Eden: "*High Energy Collisions of Elementary Particles*", Cambridge University Press (1967).
- [29] E. Gotsman, E.M. Levin and U. Maor: *Nucl. Phys.* **B464** (96) 251; *Nucl. Phys.* **B493** (97) 354.